Design and Testing of an Airbag Landing Attenuator System for a Generic Crew Return Vehicle

Michelle Cooper* and Robert Sinclair†
Irvin Aerospace Inc, Santa Ana, CA 92704

John Sanders‡
Irvin Aerospace Inc, Santa Ana, CA 92704

and

Jacapo Frigerio§
Lockheed Martin Space Systems Company, Denver, Colorado

Irvin Aerospace Inc has been involved in the design and manufacture of impact attenuation airbags for some time and has recently, in collaboration with Lockheed Martin, undertaken a program to provide technology demonstration for an impact attenuation system for a generic crew return vehicle. The program consisted of the design and manufacture of a suite of actively controlled, venting airbags, a gassing system and associated electronic sequence control hardware mounted to an 11,500lb mass simulator. The program culminated in a series of tower drop tests employing various drop heights and vehicle inclinations. The objective of the program was to provide confidence in an airbag system design when subjected to vertical velocities and a primary goal was to validate the system modeling conducted prior to the tests and to also provide confidence in extrapolating these data, as applicable, to landing scenarios involving both vertical and horizontal velocities onto varied terrain. The attenuation system consists of four main, venting airbags, each with an internal, permanently inflated airbag. The latter provides ground clearance following the initial landing impact. Incorporated into each outer, venting airbag is an orifice that allows the entrapped gas to exit the control volume. The size of the orifice is tailored to control flow rate of the exiting gas, improving the airbag stroke efficiency. The initial airbag geometry design was undertaken using the LSDYNA analysis tool which has been used extensively by Irvin to accurately predict the performance of airbags during impact. The overall performance of the attenuation system depends heavily on the mass flow rate of the gas exiting the vent. In order to accurately capture the vent discharge coefficient, a series of tests were performed within a desired pressure envelope. These tests served to both calibrate the LSDYNA landing model and determine if changes to the overall orifice size were necessary.

I. Airbag Design

The attenuation system consists of four main, venting airbags, each with an internal, permanently inflated airbag. The latter provides ground clearance following the initial landing impact. Incorporated into each outer, venting airbag is an orifice that allows the entrapped gas to exit the control volume. The size of the orifice is tailored to control flow rate of the exiting gas, improving the airbag stroke efficiency.

---

* Program Manager, Irvin Aerospace Inc, Santa Ana, CA 92704.
† Design Group Manager, Irvin Aerospace Inc, Santa Ana, CA 92704, Member AIAA.
‡ Systems Analyst, Irvin Aerospace Inc, Santa Ana, CA 92704,
§ Staff Engineer, Lockheed Martin Space Systems Company, Mail Stop S8085, P.O. Box 179, Denver, CO 80201

The initial airbag geometry design airbag geometry design was undertaken using the LSDYNA analysis tool which has been used extensively by Irvin to accurately predict the performance of airbags during impact.

An airbag system is usually optimized for a specific vehicle weight, descent velocity, and peak acceleration magnitude. Generally, the optimization routine involves trading the initial airbag pressure, acceleration trigger, and vent orifice area. A number of other variables come into play as the airbag design matures, including vent locations, potential for vent blockage, and anticipated landing envelope. A perfectly optimized airbag system for a single, vertical landing scenario would bring the vehicle to rest in a single stroke, dissipating all vertical velocity, and eliminating any vehicle rebound.

The airbag system for the impact attenuation technology demonstration was designed around the intent to exhibit representative performance to that of the actual reentry system. The fully operational reentry vehicle may encounter a high-horizontal velocity landing into a negative ground slope – the ground is sloping away from the vehicle. In this case, the vehicle is very prone to flipping. To improve the landing performance, the airbag system was designed to reduce the topple moment by quickly lowering the vehicle CG and allowing the anti-bottoming airbags to provide a restoring moment. A degree of efficiency is lost in the vertical scenarios because of the objective to quickly lower the CG. This loss of efficiency is manifested in an increase in residual impact energy, inducing a minimal rebounding effect.

The geometry of the reentry simulator was imported from a solid model of the assembly and a finite mesh of shell elements was overlaid on the structure. The appropriate shell thicknesses and material properties were assigned to the elements to capture the physical response and loading characteristics of the mass simulator.

The airbags are constructed of a high-strength, 13.25-oz/yd^2 polyurethane-coated Kevlar fabric. The primary airbag construction consists of an outer, venting airbag and an internal, permanently inflated airbag. The latter provides ground clearance following the initial landing impact. Incorporated into each outer, venting airbag is an orifice that allows the entrapped gas to exit the control volume. The size of the orifice is tailored to control flow rate of the exiting gas, improving the airbag stroke efficiency.

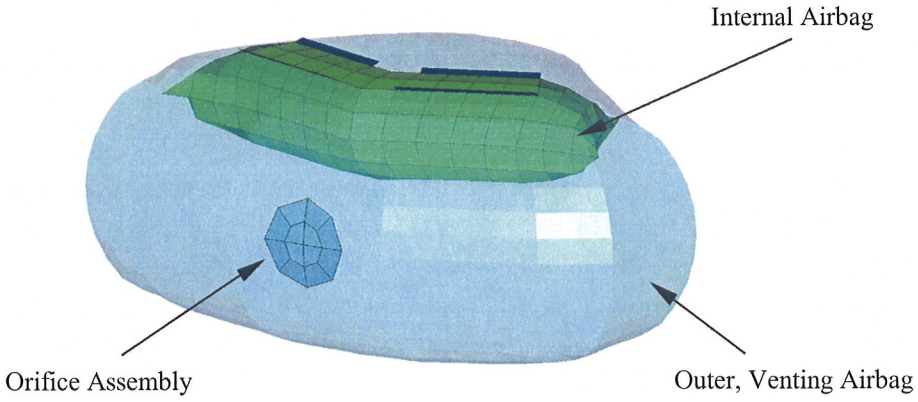

A signal to vent the primary airbags is initiated as the accelerometer mounted on the vehicle reads a predetermined acceleration magnitude. The venting is facilitated by a pyro-initiated cutter mounted on the exterior of the airbag. This technique, while adding a slight level of complexity, has been proven on numerous occasions to provide superior performance to passive venting, such as pressure based burst discs.

Several additional levels of fidelity have been incorporated into the model to filter unrealistic acceleration peaks, due to structural resonance, and electronic delays, a result of instrumentation data acquisition rates. The unrealistic acceleration peaks are filtered by establishing a time duration through which the acceleration must exceed a dictated value to verify that the vehicle is experiencing ground impact.

II. Airbag Construction

Using the airbag geometry from the preliminary simulation effort, fabric patterns were created. The figure below compares the initial simulated geometry and the final shape using the fabric pattern. The primary difference between the two designs is that the large outboard radius in the actual design has been broken into five facets to facilitate airbag production.

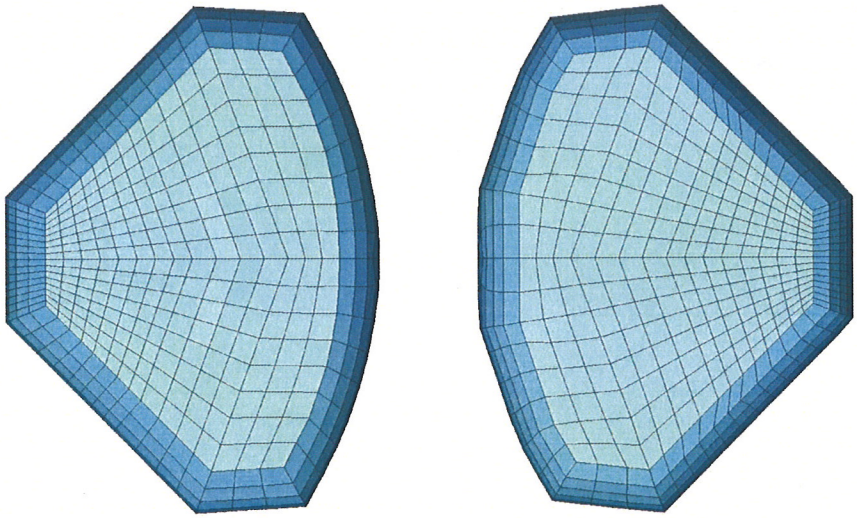

Figure 1. Airbag Construction Comparison

III. Vent Orifice Calibration

The overall performance of the attenuation system depends heavily on the mass flow rate of the gas exiting the vent. In order to accurately capture the vent discharge coefficient, a series of tests were performed, in accordance with reference 1, within a desired pressure envelope. These tests served to both calibrate the landing model and determine if changes to the overall orifice size were necessary.

Each test consisted of inflating the airbag to a dictated pressure and, using a pyro-initiated cutter, opening the vent. Several of these tests were performed at different pressures.

The results of the tests indicate that a theoretical orifice coefficient of 0.7 adequately captures the actual venting performance of the airbag. The following figures show the orifice pre and post test.

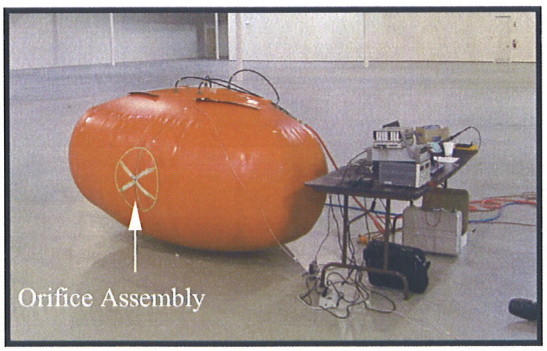

Figure 2. Pre Calibration Test

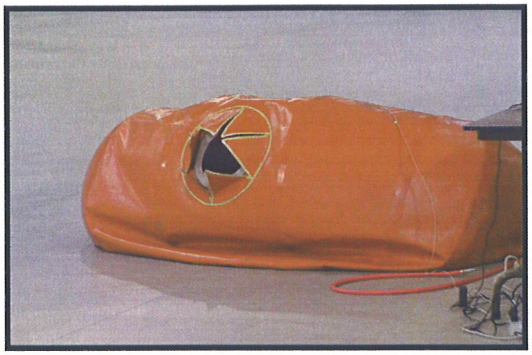

Figure 3. Post Calibration Test

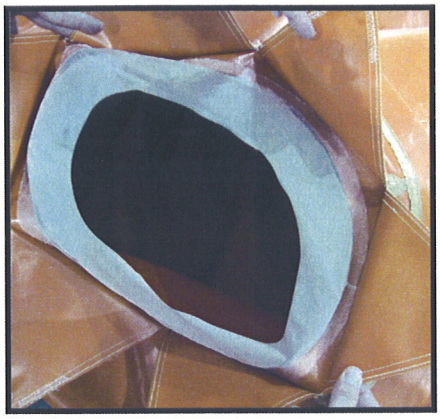

Figure 4. Orifice Post Test

IV. Airbag Venting Performance

The traces below outline the pressure-time history of the venting airbag during the tests. The calibrated pressure transducer data was used to accurately capture the true pressure-time history in the airbag. Compared in each plot are the predicted and actual pressure histories. The predicted performance is based on an orifice coefficient of 0.7. The results of these tests are detailed in reference 3.

The first two tests exhibit a very strong correlation between the actual and predicted airbag performance.

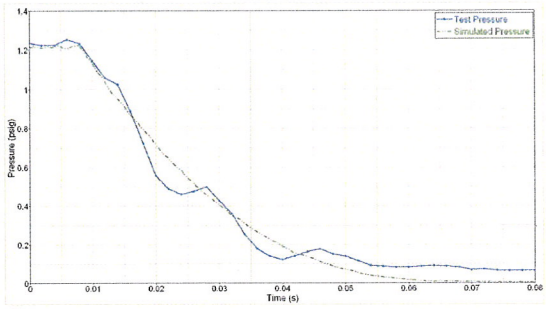

Figure 5. Test 1 Pressure vs. Time

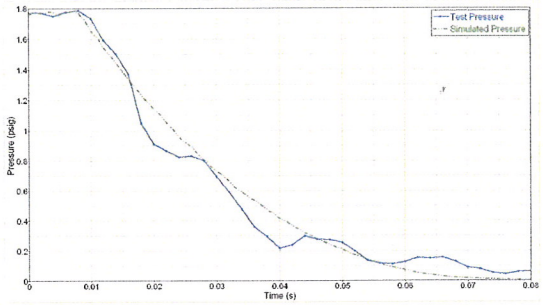

Figure 6. Test 2 Pressure vs. Time

The third test was conducted at the highest of the three pressures. Because of the single layer of fabric defining the orifice in the prototype bag, the large mass flow rate caused a small tear to form in the orifice. The tear resulted in an increase in orifice area and associated mass flow rate. Without this tear, the test and simulated pressure curves would show a much stronger correlation.

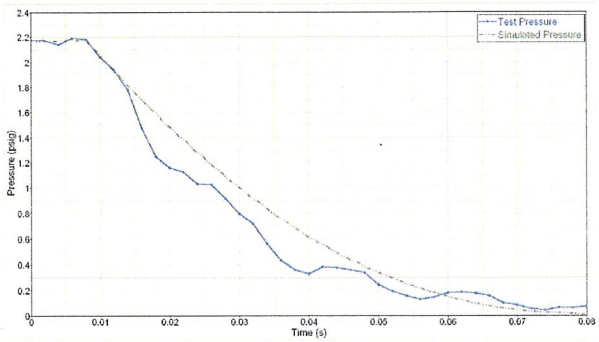

Figure 7. Test 3 Pressure vs. Time

V. Calibration Test Conclusions

A series of airbag tests were performed to both calibrate the landing model and determine if changes in the orifice area are necessary to improve landing performance. Based on the results of the test, the assumed orifice coefficient used to size the vents, 0.7, adequately captures the actual airbag venting characteristics.

VI. Simulation Results

The airbag attenuation system was optimized around a descent velocity of 22 ft/s. The intent of this airbag design is to mimic the performance characteristics desired in a full fidelity reentry vehicle recovery system. The most noticeable of these characteristics is the residual vertical velocity as the anti-bottoming airbags impact the ground in the nominal case. The majority of the impact energy has been dissipated and the remaining energy will be used to improve the crosswind performance of the fully functional reentry vehicle.

The beginning of all of the scenarios is marked with a slight increase in descent velocity as the pressure in the airbag builds and the bag contours to the shape vehicle and ground. The overall stroke efficiency is reduced because of this change in airbag shape during the initial stages of ground impact. The incorporation of shape control serves to improve the efficiency by dictating the initial impact shape; however, because of time restrictions and attachment logistics, shape control was not employed in this airbag system. The evolution of the design is presented in reference 4.

A. Scenario 1: 20 ft/s Vertical Velocity – 0° Pitch

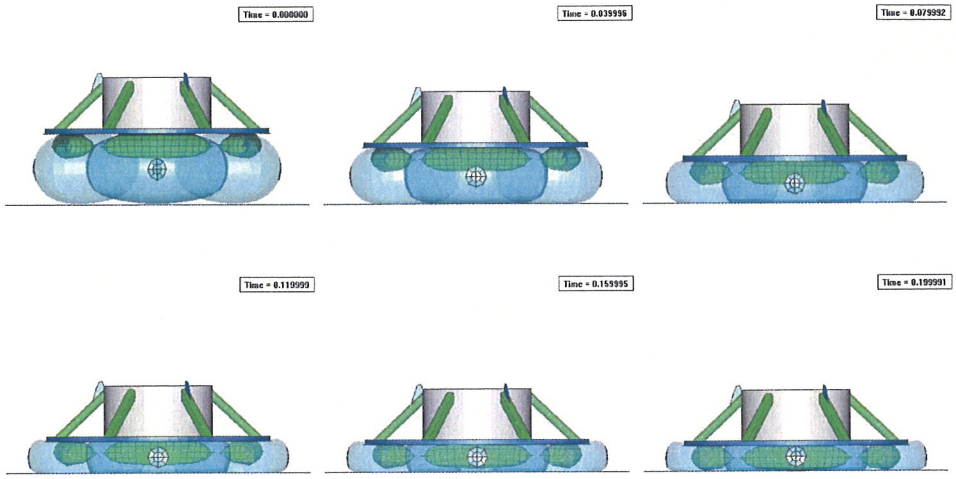

Figure 8. Landing Animation

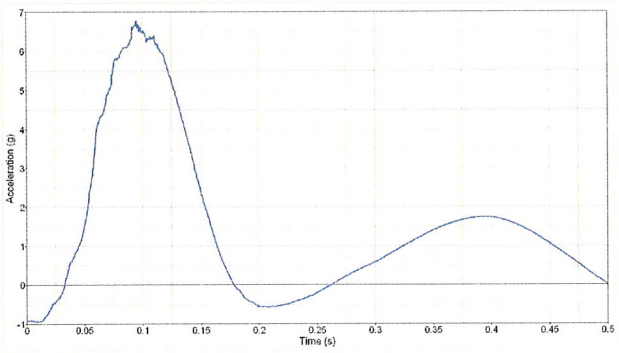

Figure 9. Acceleration Time History

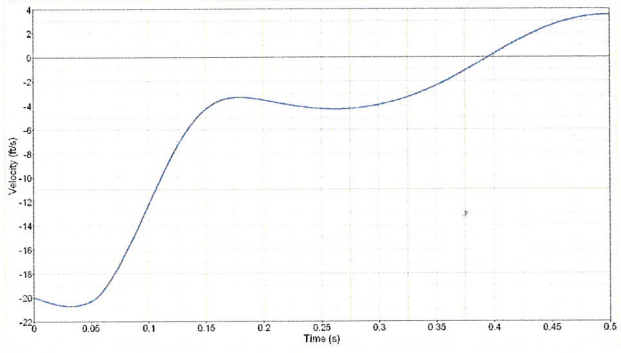

Figure 10. Velocity Time History

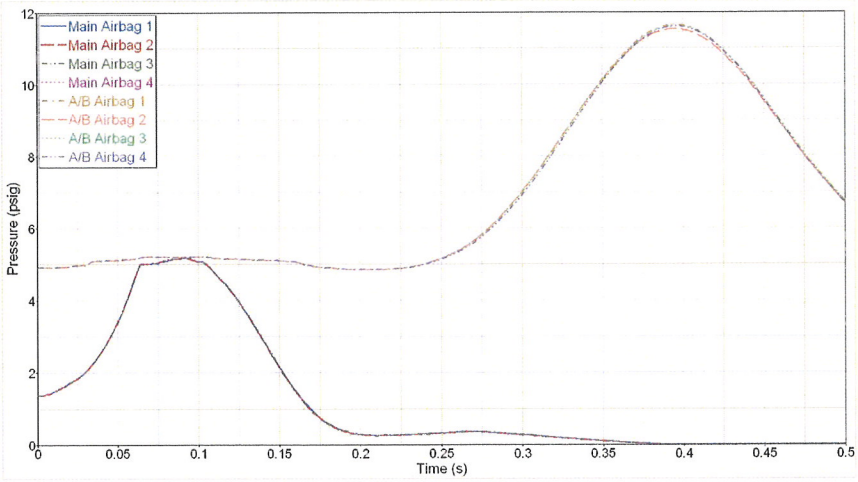

Figure 11. Airbag Pressure Time History

B. Scenario 2: 22 ft/s Vertical Velocity – 0° Pitch

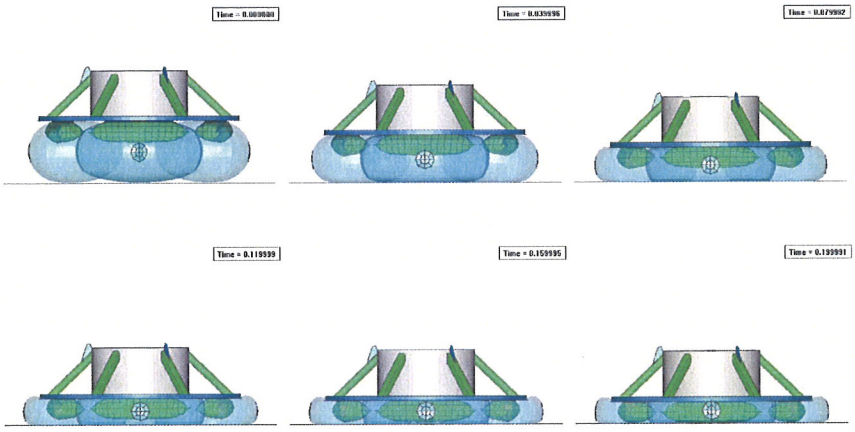

Figure 12. Landing Animation

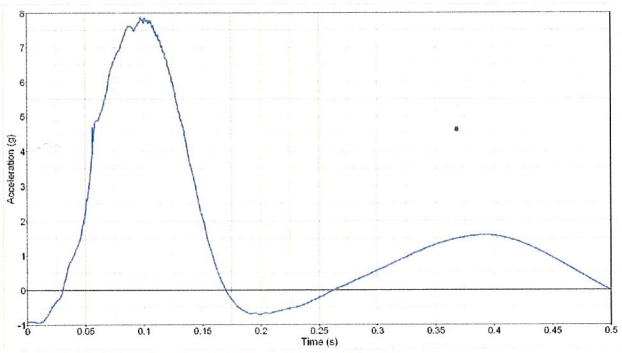

Figure 13. Acceleration Time History

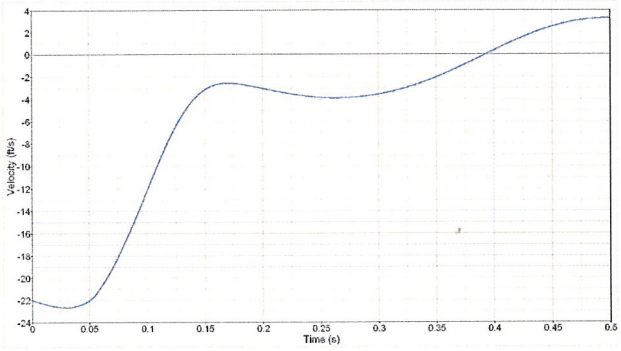

Figure 14. Velocity Time History

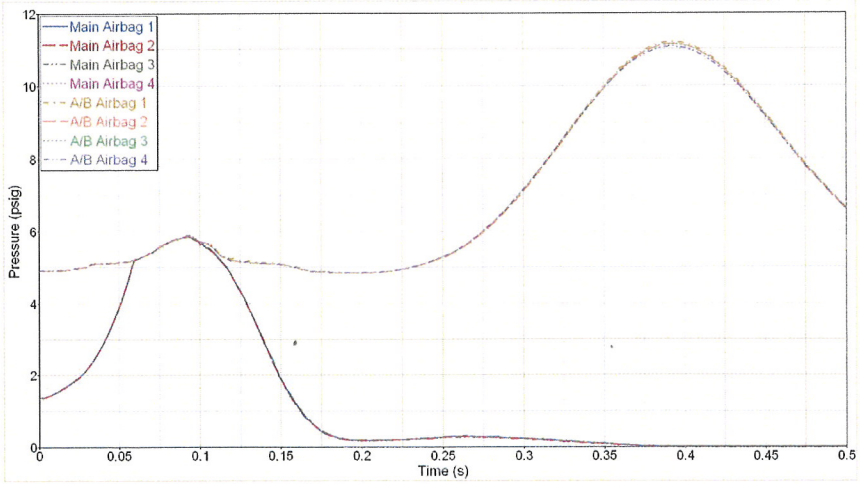

Figure 15. Airbag Pressure Time History

C. Scenario 3: 22 ft/s Vertical Velocity – 2° Pitch

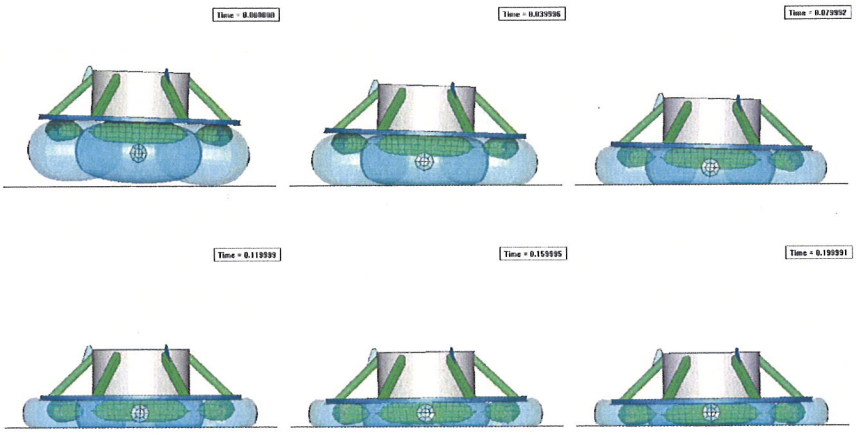

Figure 16. Landing Animation

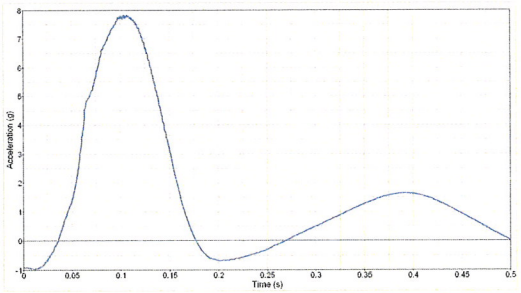

Figure 17. Acceleration Time History

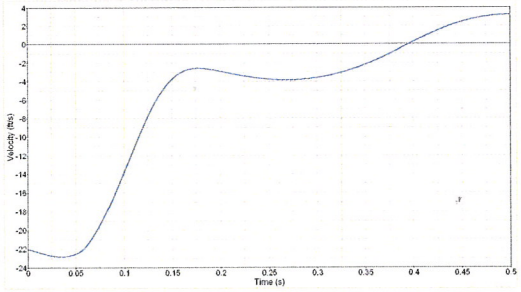

Figure 18. Velocity Time History

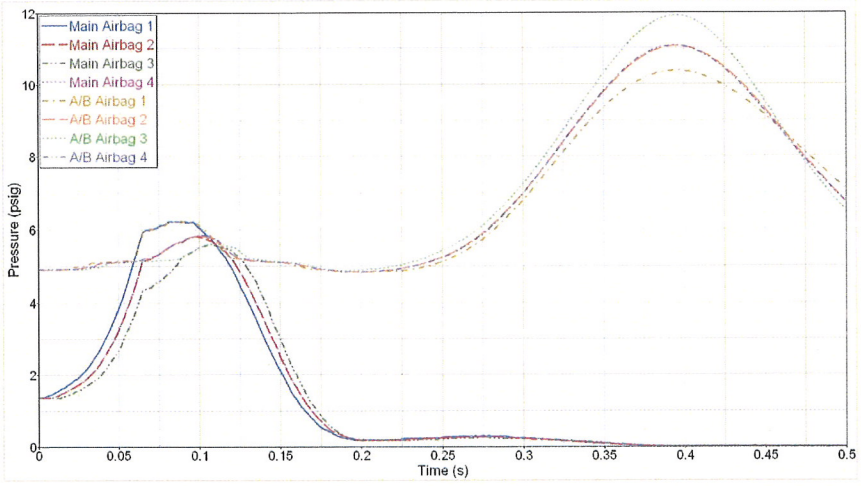

Figure 19. Airbag Pressure Time History

D. Scenario 4: 22 ft/s Vertical Velocity – 5° Pitch

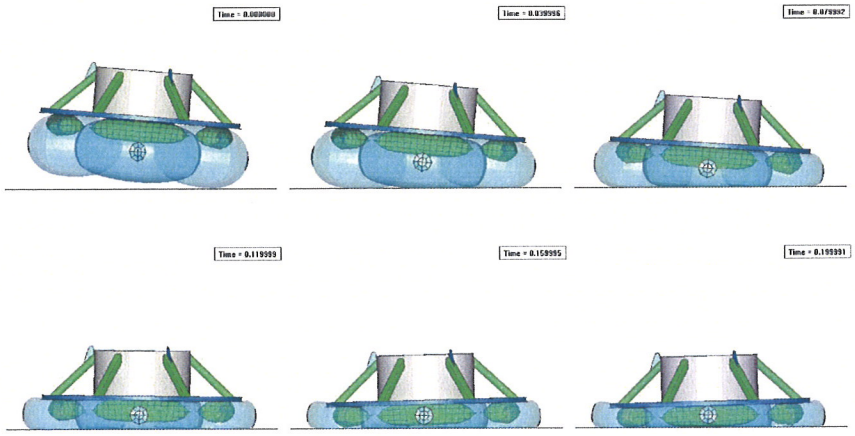

Figure 20. Landing Animation

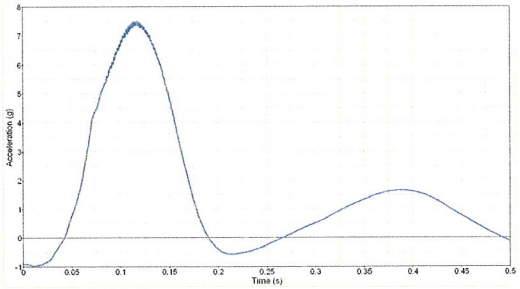

Figure 21. Acceleration Time History

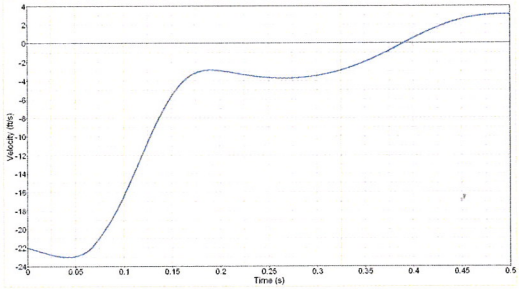

Figure 22. Velocity Time History

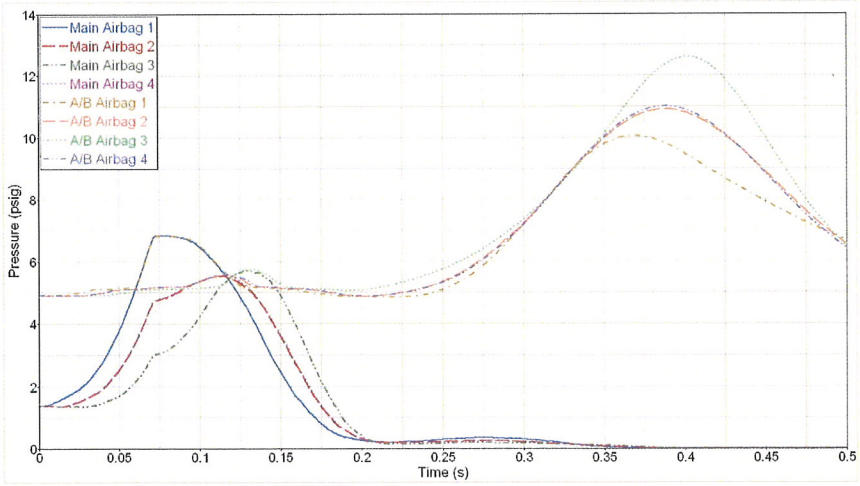

Figure 23. Airbag Pressure Time History

E. Scenario 5: 28 ft/s Vertical Velocity – 0° Pitch

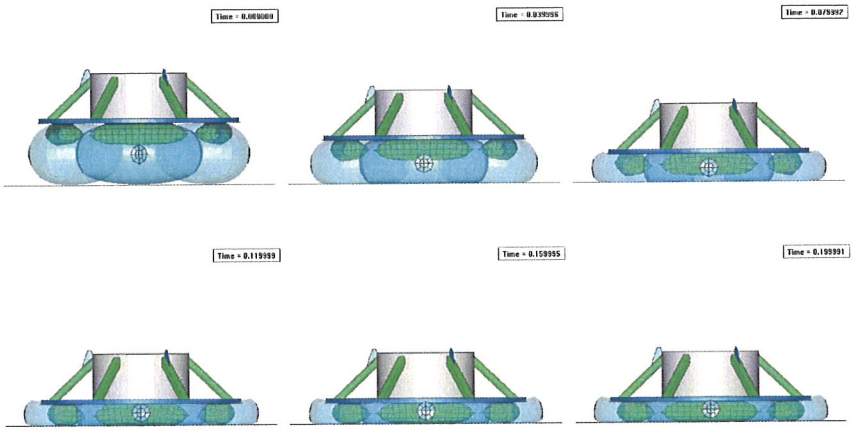

Figure 24. Landing Animation

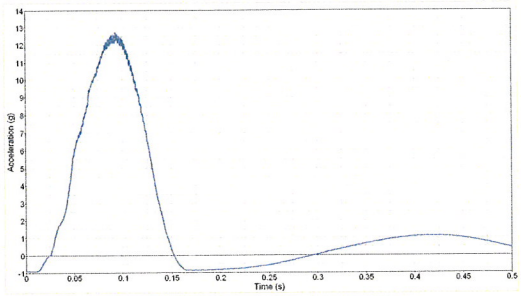

Figure 25. Acceleration Time History

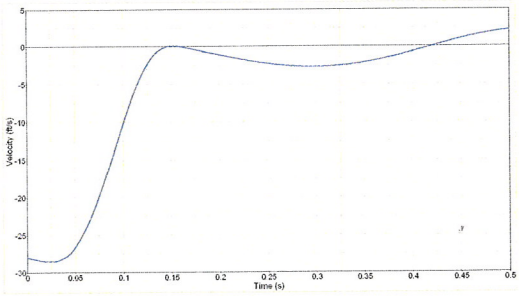

Figure 26. Velocity Time History

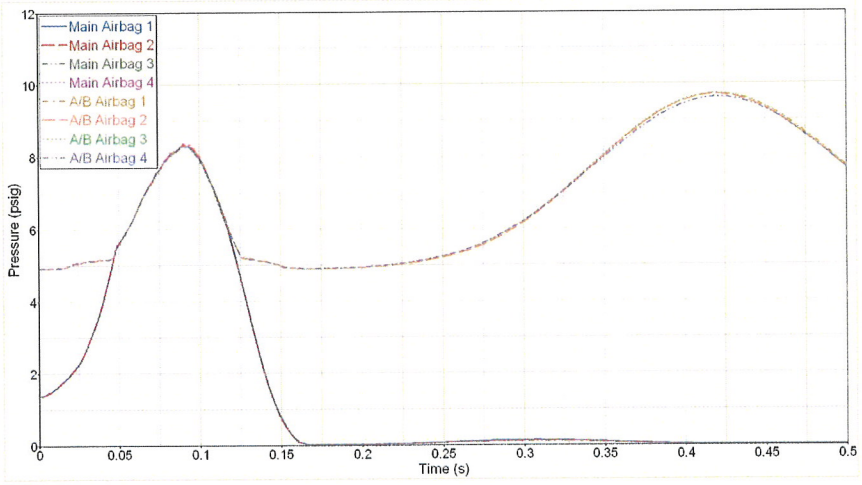

Figure 27. Airbag Pressure Time History

VII. Test Vehicle Design

F. Basic Structure

The test vehicle structure was supplied by Lockheed Martin and consisted of a steel drum mounted to a 12.5ft diameter steel plate. Support struts were used to distribute the load across the steel base plate. The empty vehicle weighed approximately 5000 lbs and sand was used to ballast the vehicle up to 11500 lbs at the test site. The test vehicle structure is shown in Figure 28.

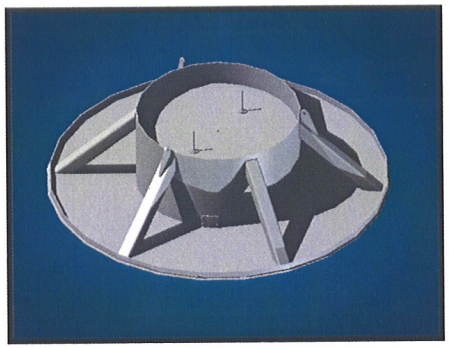

Figure 28. Test Vehicle Structure

G. Gassing System

The gassing system was employed only to supply top-up gas to the airbags during the period between initial fill and test. The primary gas supply was from shop air. The gassing system comprised of 2 filament-wound bottles that were charged with Nitrogen to 900 PSI prior to each test. Each bottle fed 2 pneumatic circuits which, in turn, fed the inner and outer supply lines. Pressure was monitored using digital pressure switches that were set to switch within a 0.5 PSI dead-band. The pressure switches operated electrical solenoid valves which controlled the flow of gas. The gassing system is shown in Figure 29.

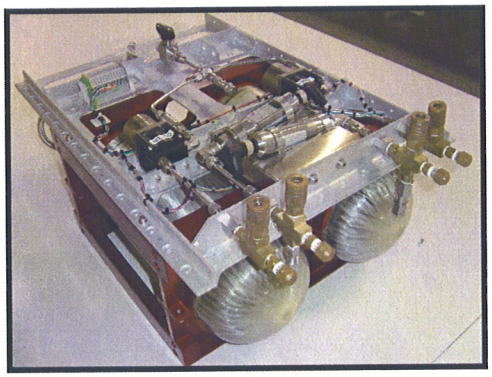

Figure 29. Gassing System

H. Sequencer

The test vehicle was controlled using a digital on-board computer system that is software driven. The sequencer continually monitored the 2 accelerometers mounted on the Z axis of the vehicle and the software was coded such that each of these accelerometers had to see the required acceleration level for a specific time period before the command signal was sent to the pyrotechnic cutters on the airbag vents. The sequencer is shown in Figure 30.

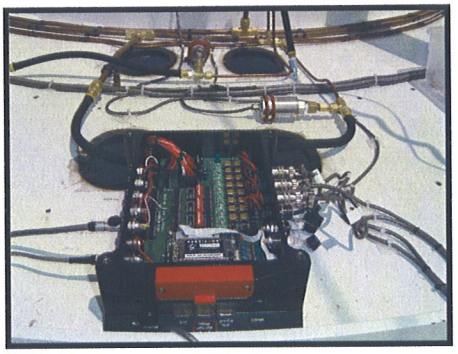

Figure 30. Sequencer

I. Instrumentation

The vehicle was instrumented with the following sensors:

8 Pressure Transducers measuring the internal pressure of the inner and outer Airbags
1 X-axis accelerometer
1 Y-axis accelerometer
2 Z-axis accelerometer
1 rate gyro measuring pitch rate
1 rate gyro measuring roll rate

All of these sensors collected the data at an acquisition rate of 1000 Hz. The data was collected directly onto a laptop computer via an umbilical from the test vehicle.

VIII. Test Setup

The tests were conducted at the US Army Yuma Proving Ground drop test facility. The test vehicle was placed on stands below the drop tower and the airbags were installed. Shop air was used to inflate the inner and outer bags to approximately 95% of the required working pressure, at which point the shop air was disconnected and inflation control was controlled by the gassing system. The vehicle was then raised to the correct height and just prior to release the data acquisition system was switched on. At release a trip switch started a timer on the sequencer which disabled the pyrotechnic firing circuit for a period of 250 ms. this time delay ensured any resonance resulting from the release event would not trigger the accelerometers and initiate the vents. The following figures show a typical test setup. The test was conducted in accordance with the plan detailed at reference 5.

Figure 31. Initial Test Setup

Figure 32. System Prior to Release

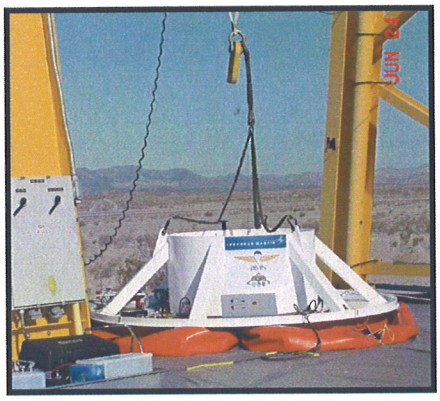

Figure 33. System Post-Test

IX. Test Results

The complete test report is detailed in reference 6. This section summarizes the test results and discusses the particular areas of interest for each of the 5 tests.

J. Test 1 ~ Zero Degree Angle of Incidence, Impact Velocity 20ft/s

1. Test Conditions

Date: Thursday 24th June 2004 approximately 11:00 a.m.
Temperature: 87° F
Humidity: 21% RH
Wind: Nominally 6 knots

K. Recorded Data, Test 1

The table below presents a summary of the recorded data. As the test was at a zero degree angle of incidence, where appropriate, the peak values presented below are an average of the data gathered for all four airbags.

Detailed graphical data is shown below.

Description	Test Data
Peak Velocity	20.0 ft/s
Peak Main Airbag Pressure	5 psig
Peak Anti-bottoming Bag Pressure	10 psig
Peak Acceleration	4.9 g

L. Main Airbag Pressure v Time, Test 1

Figure 34 presents Main Airbag Pressure v Time. The simulation results are also shown.

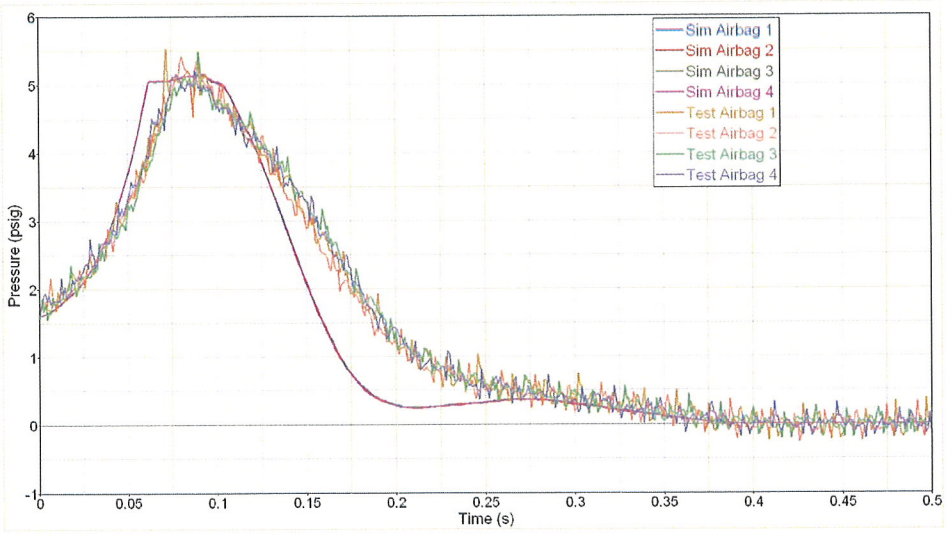

Figure 34. Main Airbag Pressure v Time

M. Anti-Bottoming Airbag Pressure v Time, Test 1

Figure 35 presents Anti-Bottoming Airbag Pressure v Time. The simulation results are also shown.

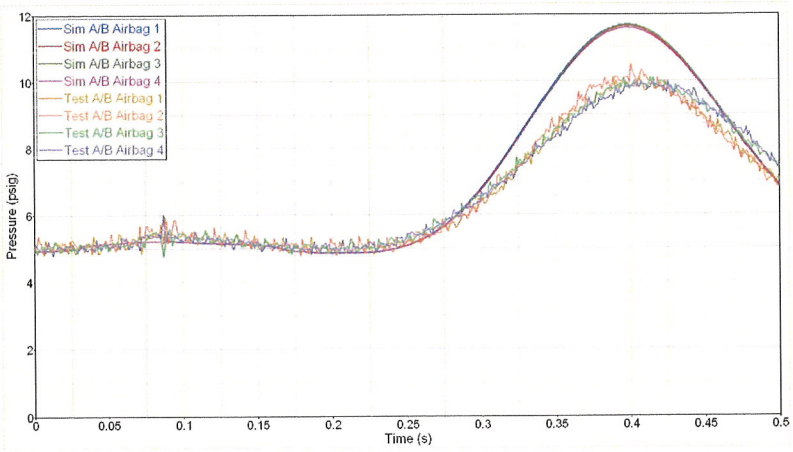

Figure 35 ~ Anti-Bottoming Airbag Pressure v Time

N. Acceleration v Time, Test 1

Figure 36 presents Acceleration v Time. The simulation results are also shown.

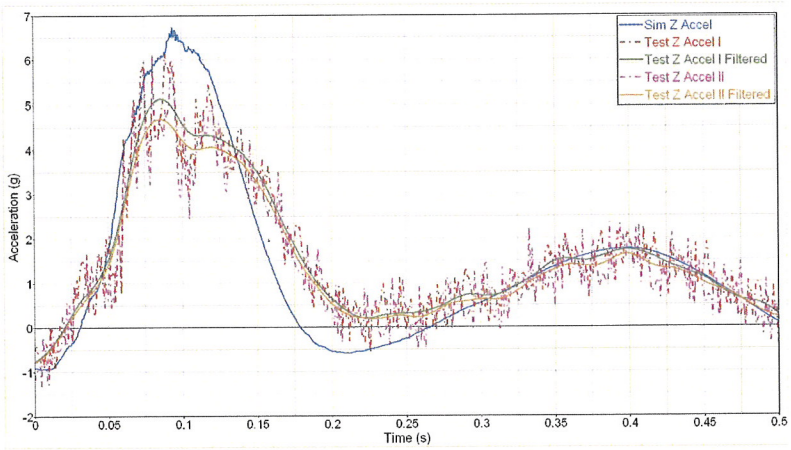

Figure 36 ~ Acceleration v Time

O. Discussion, Test 1

The peak predicted acceleration is approximately 6.5 g, while the recorded data from the accelerometers indicated a peak acceleration of approximately 5 g, factoring out some of the instrumentation and resonance noise. Note that the primary impact stroke is completed over approximately 200 ms.

The pressures among all of the main airbags follow closely, indicating the consistency between the construction and performance of the bags. Similarly, all of the anti-bottoming airbags also demonstrate consistent performance.

The main airbags in the test exhibit a slightly less dramatic drop in pressure as the airbags vent as compared to the predicted performance. The second peak in the acceleration time history occurs as the anti-bottoming airbags reacted against the ground. The overall acceleration as the anti-bottoming airbags reach the ground matches closely, however, the peak pressure is slightly lower than predicted.

The vehicle-mounted accelerometers may have encountered a harmonic during the landing event, as a result of the flex of the base plate. The first order harmonic of the base plate on the vehicle is approximately 10 Hz. This resonance can be observed during the initial impact pulse. In this test, the harmonic does not introduce an unrealistically large acceleration peak and is quickly damped by the ballast sand. In other tests, this resonance becomes much more pronounced and the local acceleration does not completely represent the rigid body acceleration of the vehicle. In order to reduce the influence of this harmonic, the data was filtered at 10 Hz.

Immediately after ground impact, the mass simulator tended to bounce on the anti-bottoming bags until the action was damped. This phenomenon was predicted through the simulation, as the system was optimized for a higher impact energy landing. The lower energy landing results in a loss in airbag stroke efficiency.

P. Test 2 ~ Zero Degree Angle of Incidence, Impact Velocity 22ft/s

Test Conditions, Test 2

Date: Thursday 24th June 2004 approx. 4.30pm.
Temperature: 105° F
Humidity: 13% RH
Wind: Nominally 6 knots

Q. Recorded Data, Test 2

The table below presents a summary of the recorded data. As the test was at a zero degree angle of incidence, where appropriate, the peak values presented below are an average of the data gathered for all four airbags.

Detailed graphical data is shown below.

Description	Test Data
Peak Velocity	21.6 ft/s
Peak Main Airbag Pressure	6.2 psig
Peak Anti-bottoming Bag Pressure	9.5 psig
Peak Acceleration	7.5 g

R. Main Airbag Pressure v Time, Test 2

Figure 37 presents Main Airbag Pressure v Time. The simulation results are also shown.

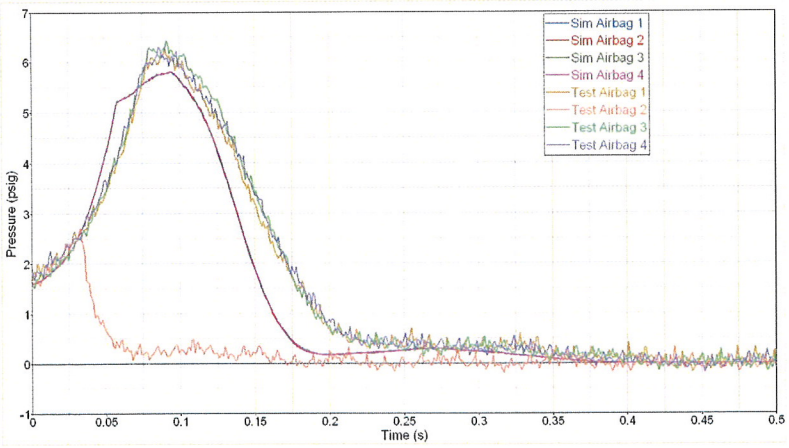

Figure 37 ~ Main Airbag Pressure v Time

S. Anti-Bottoming Airbag Pressure v Time, Test 2

Figure 38 presents Anti-Bottoming Airbag Pressure v Time. The simulation results are also shown.

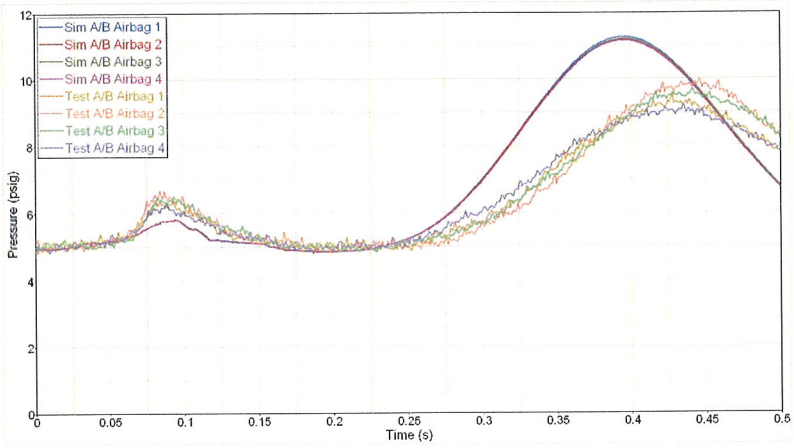

Figure 38 ~ Anti-Bottoming Airbag Pressure v Time

T. Acceleration v Time, Test 2

Figure 39 presents Acceleration v Time. The simulation results are also shown.

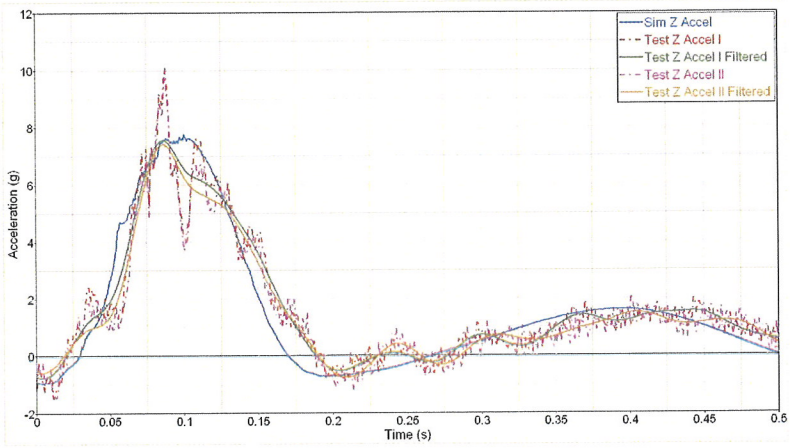

Figure 39 ~ Acceleration v Time

U. Discussion, Test 2

A single quick-release on a sense line disconnected during the primary impact (airbag 2), eliminating a single channel of data. This test is the only instance when a sense line was lost.

The base plate began to resonate during the primary impact. The local acceleration peaks recorded by the accelerometers are higher than the rigid body acceleration of the vehicle, indicated by the sharp rebound in the acceleration trace. The ballast sand damps this resonance after several cycles. Another indication that the resonance is a local phenomenon is the main airbag pressure traces – the pressures in the main airbags do not follow the dramatic rebound recorded by the accelerometer.

Immediately after ground impact, the mass simulator tended to bounce on the anti-bottoming bags until the action was damped.

V. Test 3 ~ 3.3° Angle of Incidence, Impact Velocity 22ft/s

Test Conditions, Test 3

Date: Friday 25th June 2004 approx. 11am.
Temperature: 105° F
Humidity: 7% RH
Wind: Nominally 5 knots

W. Recorded Data, Test 3

The table below presents a summary of the recorded data. As this test was configured for the 3.3-degree angle of incidence, where appropriate, the peak values presented below represent the data from the leading airbag.

Detailed graphical data is shown below.

Description	Test Data
Peak Velocity	22.3 ft/s
Peak Main Airbag Pressure	6.7 psig
Peak Anti-bottoming Bag Pressure	10.4 psig
Peak Acceleration	7.2 g

X. Main Airbag Pressure v Time, Test 3

Figure 40 presents Main Airbag Pressure v Time. The simulation results are also shown.

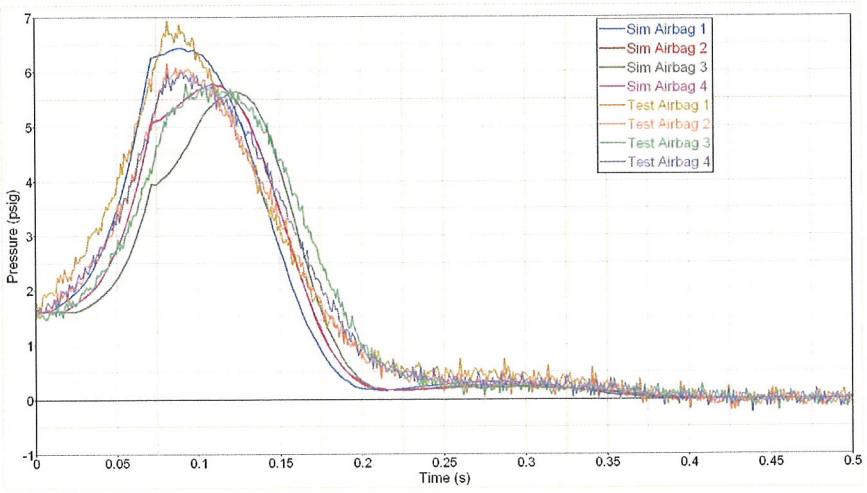

Figure 40 ~ Main Airbag Pressure v Time

Y. Anti-Bottoming Airbag Pressure v Time, Test 3

Figure 41 presents Anti-Bottoming Airbag Pressure v Time. The simulation results are also shown.

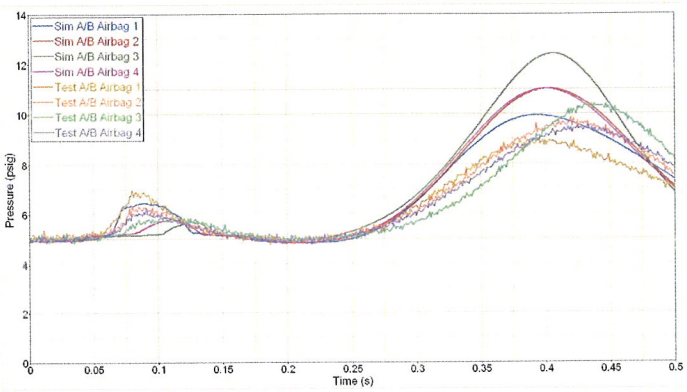

Figure 41 ~ Anti-Bottoming Airbag Pressure v Time

Z. Acceleration v Time, Test 3

Figure 42 presents Acceleration v Time. The simulation results are also shown.

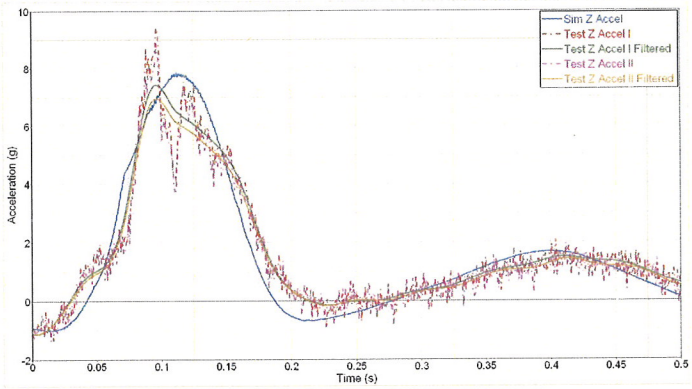

Figure 42 ~ Acceleration v Time

AA. Angular Velocity v Time, Test 3

Figure 43 presents Acceleration v Time. The simulation results are also shown.

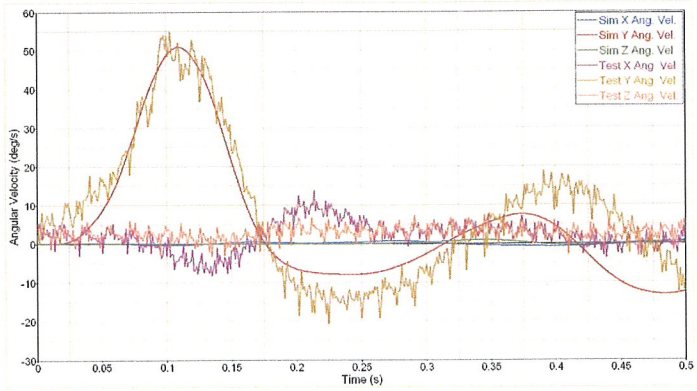

Figure 43 ~ Angular Velocity v Time

BB. Discussion, Test 3

Again in this test, the accelerometers recorded relatively high acceleration peaks followed by a sharp valley, symptomatic of a harmonic. This distinct acceleration history does not appear in the pressure traces, indicating that the accelerometers are recording a local acceleration phenomenon.

CC. Test 4 ~ 8.3° Angle of Incidence, Impact Velocity 22ft/s

Test Conditions, Test 4

Date: Friday 25th June 2004 approx. 4.30pm.
Temperature: 105° F
Humidity: 7% RH
Wind: Nominally 5 knots

DD. Recorded Data, Test 4

The table below presents a summary of the recorded data. Elongation of the harnesses resulted in an increase in a higher angle of incidence than originally required. The resulting incidence angle was measured at 8.3 degrees. The simulation was re-configured to use this incidence angle, the peak values presented below represent the data from the leading airbag.

Detailed graphical data is shown below.

Description	Test Data
Peak Velocity	22.0 ft/s
Peak Main Airbag Pressure	5.7 psig
Peak Anti-bottoming Bag Pressure	10.5 psig
Peak Acceleration	5.3 g

EE. Main Airbag Pressure v Time, Test 4

Figure 44 presents Main Airbag Pressure v Time. The simulation results are also shown.

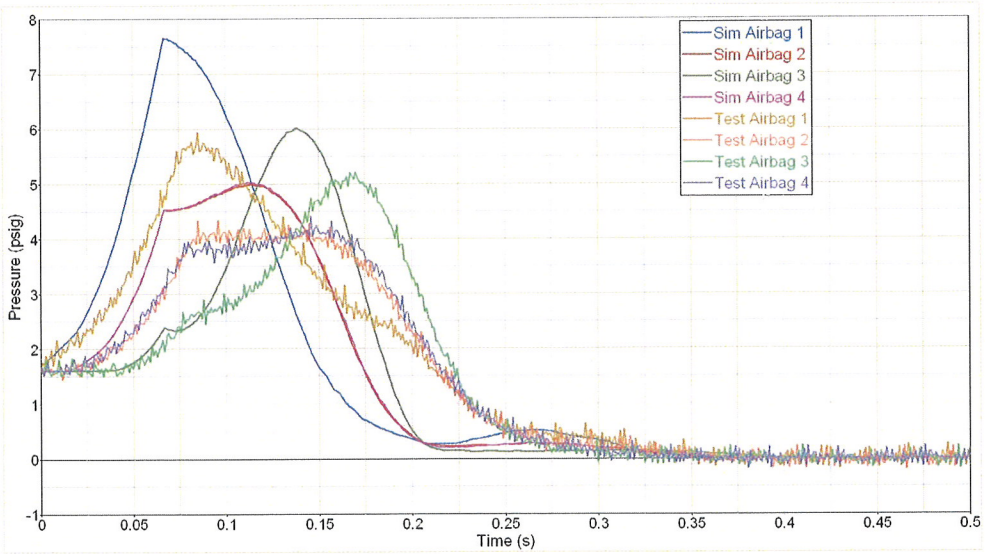

Figure 44 ~ Main Airbag Pressure v Time

FF. Anti-Bottoming Airbag Pressure v Time, Test 4

Figure 45 presents Anti-Bottoming Airbag Pressure v Time. The simulation results are also shown.

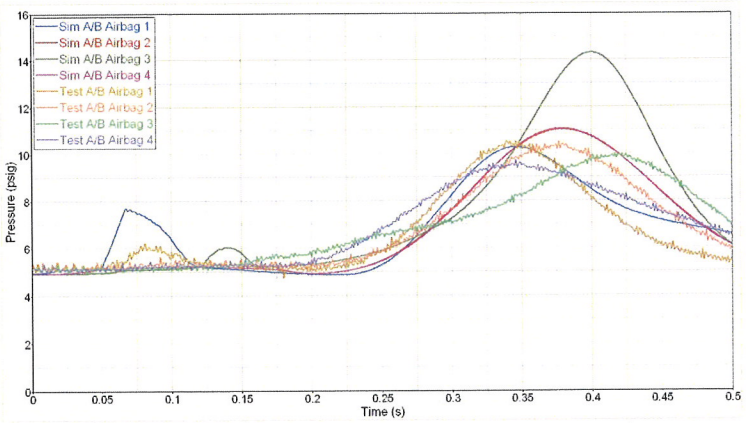

Figure 45 ~ Anti-Bottoming Airbag Pressure v Time

GG. Acceleration v Time, Test 4

Figure 46 presents Acceleration Pressure v Time. The simulation results are also shown.

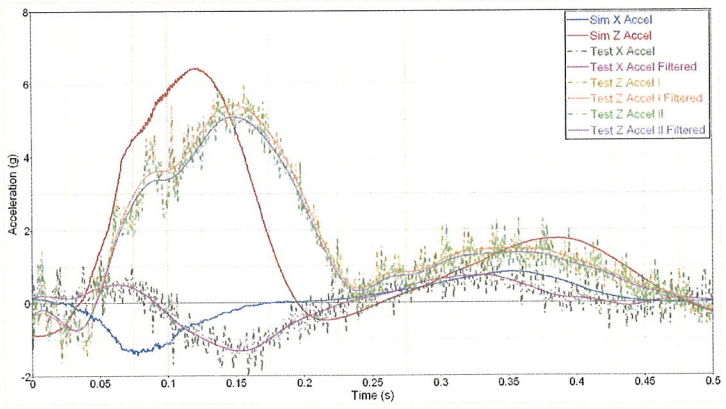

Figure 46 ~ Acceleration v Time

HH. Angular Velocity v Time, Test 4

Figure 47 presents Angular Velocity v Time. The simulation results are also shown.

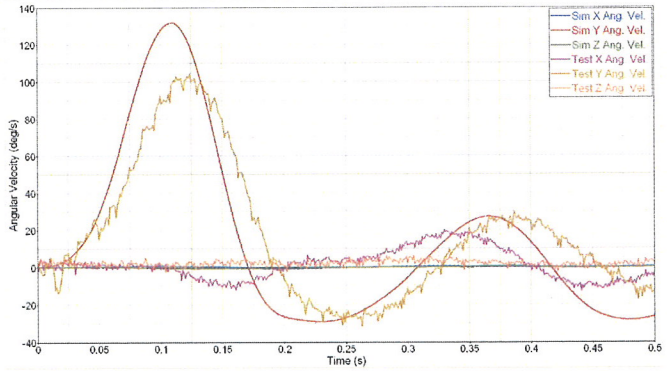

Figure 47 ~ Angular Velocity v Time

II. Discussion, Test 4

The airbag pressure curves for the 8° landing condition do not follow the prediction very closely. There is also an offset in the acceleration time history.

Several variables could explain the discrepancy. The main driver in the discrepancy is the difference in the onset of pressure in airbag 1. In the test, the pressure in airbag 1 builds much more slowly than anticipated, which may be attributed to the simulated flaps and contact considerations. Another variable is the difference between the true and predicted inflated shape. The true inflated shape appears to have a more rounded shape at the bottom of the airbag, the area that contacts the ground first. This shape would reduce the overall rate of pressure onset and allow the remaining airbags to accommodate the trigger acceleration prior to the first impact bag building the higher, predicted pressure.

Overall, the loads and accelerations encountered on the system are lower than predicted.

JJ. Test 5 ~ Zero Degree Angle of Incidence, Impact Velocity 28ft/s

Test Conditions, Test 5

Date: Friday 25th June 2004 approx. 7.00pm.
Temperature: 105° F
Humidity: 7% RH
Wind: Nominally 5 knots

KK. Recorded Data, Test 5

The table below presents a summary of the recorded data. As the test was at a zero degree angle of incidence, where appropriate, the peak values presented below are an average of the data gathered for all four airbags.

Detailed graphical data is shown below.

Description	Test Data
Peak Velocity	27.6 ft/s
Peak Main Airbag Pressure	6.6 psig
Peak Anti-bottoming Bag Pressure	7.8 psig
Peak Acceleration	10 g

LL. Main Airbag Pressure v Time, Test 5

Figure 48 presents Main Airbag Pressure v Time. The simulation results are also shown.

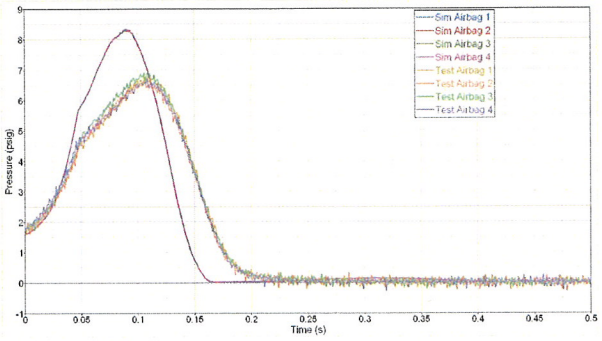

Figure 48~ Main Airbag Pressure v Time

MM. Anti-Bottoming Airbag Pressure v Time, Test 5

Figure 49 presents Anti-Bottoming Airbag Pressure v Time. The simulation results are also shown.

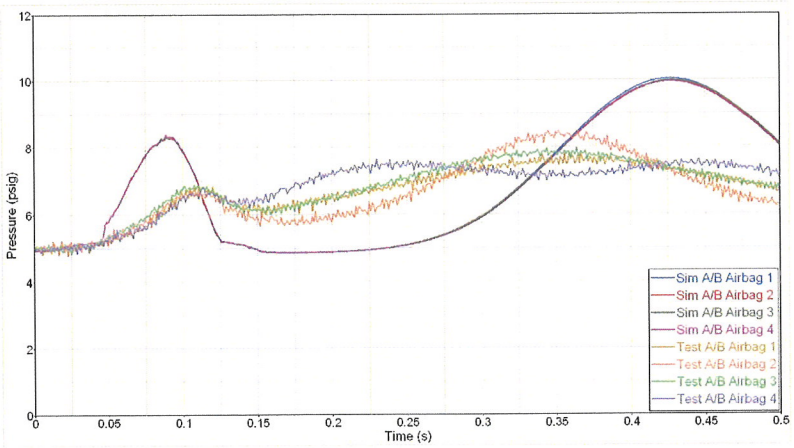

Figure 49~ Anti-Bottoming Airbag Pressure v Time

NN. Acceleration v Time, Test 5

Figure 50 presents Acceleration v Time. The simulation results are also shown.

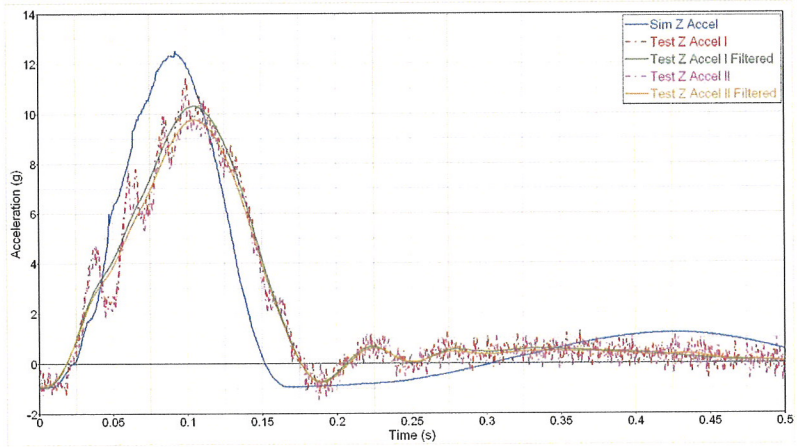

Figure 50 ~ Acceleration v Time

OO. Discussion, Test 5

In this final test, the pressure history of the main airbags differs from the pre-test prediction. This discrepancy is attributed to a variation in the orifice coefficient as the airbag strokes. Once the airbags begin to vent, the rise in pressure is less pronounced than predicted, suggesting an increase in orifice coefficient, which could be coning phenomenon or an expansion in the orifice due to strain in the surrounding fabric. However, as the pressure begins to decrease, the orifice coefficient appears to decrease and the pressure drop is less dramatic than the prediction.

The overall performance in this scenario illustrates the versatility of an airbag system in emergency scenarios.

X. Conclusions

This design effort and test campaign demonstrated the feasibility of landing relatively large Crew/Cargo Return Vehicles on hard surfaces without the use of wings, wheels, and/or retrorockets. The acceleration loads imparted into the vehicle can be managed to a tolerable level even in the case where a descent parachute, within a typical cluster, has failed and the rate of descent is in the order of 28 ft/s.

Simulation validation is an area which requires further study. There are varying degrees of mis-match in the airbag pressure time histories between the simulation and test data. Irvin are currently investigating the cause of the disagreements and are studying various possible causes, these include:

1. Variation in the discharge coefficient of the vent during landing stroke, caused by deformation of the orifice.
2. Potential blockage or partial blockage of the vent during the landing stroke.
3. Variation in the predicted inflated shape versus actual.
4. Variation in the hysteretic behavior of the airbag material due to repeated use.
5. Interaction of the pressure transducers during the landing stroke.

XI. Acknowledgements

The authors would like to thank the Lockheed Martin team members, especially John Hodge and Michelle Butzke, for their efforts during the conception and undertaking of this project. They would also like to recognize the outstanding support provided by Pat Serani, John Cordera, Paul Mortaloni and, all the staff at Yuma Proving Ground that helped to ensure the success of this project.

XII. References

[1]Cooper, M.S., Taylor, A.P., Farhall, R.J., Irvin document GIP 99-1100 Test Plan for Initial System Testing

[2]Cooper, M.S., Farhall, R.J., Irvin document GIP 99-1091 Test Procedure for Airbag Orifice Testing

[3]Sanders, J., Cooper, M.S., Taylor, A.P., Irvin Document GIR 93-198 Airbag Orifice Test and Simulation Calibration Report

[4]Sanders, J., Cooper, M.S., Taylor, A.P., Irvin Document GIR 85-1331 Analysis and Design Evolution Report for the Lockheed Martin Reentry Vehicle Simulator Airbag Attenuation System

[5]Cooper, M.S., Taylor, A.P., Farhall, R.J., Irvin Document GIP 99-1089 Test Plan for Impact Attenuation Testing at Yuma Proving Ground

[6]Sanders, J., Cooper, M.S., Taylor, A.P., Farhall, R.J., Irvin Document GIR 93-201 Test Report for Airbag Impact Attenuation Testing at Yuma Proving Ground